ILASS 2008
Sep. 8-10, 2008, Como Lake, Italy

Paper ID ILASS08-2-1

INFLUENCE OF SPECIES CONCENTRATION ON THE EVAPORATION OF SUSPENDED MULTICOMPONENT DROPLETS

George Strotos*, Manolis Gavaises°,§, Andreas Theodorakakos+ , George Bergeles*

*National Technical University of Athens, Department of Mechanical Engineering
5 Heroon Polytechniou, 15710 Zografos, Athens, Greece
°City University London, School of Engineering and Mathematical Sciences
Northampton Square, EC1V 0HB, London, UK
+Fluid Research Co. 49 Laskareos Str, 11472, Athens, Greece
§Correspondence author email: m.gavaises@city.ac.uk

ABSTRACT

The evaporation of droplets consisting from n-heptane, n-decane and mixture of the two at various concentrations is examined numerically. Droplets are held in suspension at the end of a small diameter pipe in a hot air environment under convective flow conditions. For predicting the temperature of the droplet and its evaporation rate as function of time the Navier-Stokes equations are solved numerically coupled with the VOF methodology for tracking the droplet interface using an adaptive local grid refinement technique. Furthermore, the energy and concentration equations inside the liquid and the gaseous phases for each of the components are solved. The model has been first validated against experimental data available in literature. Then, results from parametric studies are presented showing the effect of species composition on the internal flow field, vapour concentration and evaporation rate.

INTRODUCTION

Numerous theoretical studies have been reported in the literature on droplet evaporation, for example [1-3] among many others while more recent extended reviews are those of [4-7]. In [8, 9] one of the first droplet evaporation model was proposed, widely known as 'D^2-law' because it predicts that the squared diameter of the droplet is reduced linearly with time, while the droplet's temperature remain constant in time and space. The temporal evolution of droplet's temperature was modelled in [10] proposing the infinite conductivity model (ICM) which assumes that the droplet's temperature is changing in time but not in space. Later, in [11] which furthermore assumes that the temperature of the droplet is changing along the droplet radius, the finite conductivity model (FCM) was proposed. The effect of Stefan flow and internal circulation in the liquid phase were included in [12]. Modelling of Stefan flow was achieved by correcting heat and mass transfer numbers and the internal liquid circulation was modelled proposing the effective conductivity model (ECM), which combines the FCM with a corrected thermal conductivity that takes into account the internal liquid circulation. In [13, 14] a quite detailed analysis of the flow field both in the gas and the liquid phases was performed, by solving numerically the Navier-Stokes equations and assuming spherical droplet shape, while correlations for the Nusselt and Sherwood numbers including the effect of Stefan flow were proposed.

The modelling of multi-component droplet evaporation becomes essential, because in most practical applications fuels consist of several components. The liquid phase properties depend not only on the temperature but also on the concentration, which result in a complicated phenomenon. Different evaporation rates of each component, result in the formation of concentration gradients inside the liquid and in combination with the internal liquid circulation, it is often observed that the most volatile component is entrapped inside the liquid core towards the droplet centre. Under certain circumstances, this phenomenon can lead to micro-explosion and droplet fragmentation ([15]).

In the work of [16] the combustion of a multi-component droplets has been investigated while the Infinite Diffusivity Model (IDM) has been proposed. The Finite Diffusivity Model (FDM) was proposed by [17] and the possibility of appearance of micro-explosion was examined. The numerical solution of Navier-Stokes equations for a mixture consisting of equal amounts of n-octane and benzene has been simulated in [18] in a 2-dimensional axisymmetric geometry. The preferential evaporation of the more volatile species was observed, which it was also entrapped inside the centre of the internal recirculation zone. The work of [19] has demonstrated that for mixtures in which the more volatile component is also characterized by higher latent heat of vaporization, it is possible for a poorer in volatile species mixture to evaporate faster than a richer one, due to the higher heating of the droplet.

A moving deformable interface has been treated using various methodologies, such as the VOF methodology resulting in more complicated heat and mass transfer mechanisms. The impact and solidification of droplets onto a substrate were modelled in [20-24]. Furthermore, [25, 26] modelled the impact of droplets in hot substrate for a wide range of substrate temperatures and Weber numbers by coupling the VOF methodology with a one-dimensional heat transfer model in the sub layer between the droplet and the solid wall. The vapour layer height and the droplet levitation from the wall surface was predicted in [27] by solving numerically the Navier-Stokes equations. The vaporization of a stable droplet in contact with a heated wall was examined up to full vaporization in [28]. In this study, the Navier-Stokes equations were coupled with an evaporation model

which is independent of the flow conditions and the shape of the gas-liquid interface.

The present paper represents an extension of the work reported recently by the authors in [29], and accounts for the evaporation of a multi-component droplet suspended in a cross flow air of higher temperature. The next section of the paper describes the test case simulated, followed by a description of the numerical model. The results follow while the most important conclusions are summarised at the end.

DESCRIPTION OF TEST CASES SIMULATED

The mathematical model used, has been first validated against experimental data of [30], showing good agreement in a recent paper [29]. In these experiments, suspended droplets consisting of pure n-decane, pure n-heptane as well as mixtures of the two were subjected successively to natural and forced convection. The droplet was suspended at the spherical head (400μm) of a capillary tube (200μm), under atmospheric pressure. In the present study droplets with 1 mm diameter and 300K initial temperature are examined in a convective environment of 350K temperature, under atmospheric pressure and 3.2m/s free stream velocity. Five initial mass concentrations of n-heptane in liquid are studied; 100% (pure heptane), 75%, 50%, 25% and 0% (pure decane). The case with 75% mass concentration is considered as the reference case.

MATHEMATICAL MODEL

The mathematical model used, has been presented in detail in a recent paper [29] and will not be repeated here. Briefly, the Navier-Stokes equations are solved, coupled with an equation for the transport of the liquid-gas interface.

In order to identify each phase separately, a volume fraction is introduced and it is denoted by α, following the Volume of Fluid (VOF) method initially proposed by [31] and further developed by [32]. In this methodology the volume fraction α is defined as:

$$\alpha = \frac{\text{liquid volume}}{\text{total cell volume}} \tag{1}$$

where the α-function is 0 in the gas phase, 1 in the liquid phase and lies between 0 and 1 in the cells containing the interface area. The surface tension force is added as source term in the momentum equations, following [33].

The flow field is solved numerically on an unstructured grid using an adaptive local grid refinement technique, described in detail by [34]. Details for the discretisation of the above mentioned equations can be found in [35]. Additionally, the transport equations for energy, vapour species and liquid concentration are solved. Those equations are reported in [29], but due to its importance, the energy transport equation will be mentioned and discussed in detail later:

$$\rho c_p \frac{DT}{\mathrm{D}t} = \nabla \cdot (k \nabla T) - \sum_k \dot{m}^*_{evap,k} L_k + \nabla \cdot \left(\sum_k \rho c_{P,k} T D_{k,m} \nabla Y_k \right) \tag{2}$$

Cell properties are calculated according to [29], [35] and a similar approach is used to calculate the properties of liquid and gas phases [29].

The evaporation rate, which is independent of the interface shape, is related to Fick's law using the local concentration gradient in the interface as the driving force and assuming that the interface is saturated. The numerical results presented here have been obtained using the GFS code which has been also used in [27-29, 35, 36].

In Figure 1, the computational grid at the beginning of the simulation and the boundary conditions used are shown. The flow can be considered as two-dimensional and axisymmetric. The spherical extremity is modelled with an unstructured base grid while two levels of local grid refinement are used to enhance the spatial resolution around the gas-liquid interface.

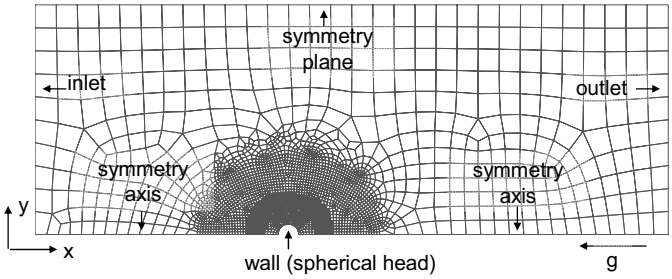

Figure 1: Computational grid and boundary conditions [29].

At the inlet of the computational domain, boundary conditions of constant velocity and temperature, dry air and zero 1st gradient for the pressure are assumed. At the outlet of the computational domain a zero 1st gradient boundary for all variables is assumed, except for pressure, which is assumed to be equal to atmospheric. Northern and southern boundaries are assumed to be a symmetry plane and a symmetry axis respectively, which corresponds to a zero 1st gradient boundary condition for all variables, except of the velocity normal to the boundary which is set to zero. Finally, the spherical head is assumed to be adiabatic impermeable wall. As initial condition for the droplet, a uniform temperature and liquid concentration is assumed.

RESULTS & DISCUSSION

Influence of concentration

In Figure 2 the temporal evolution of the droplet's squared diameter and droplet's mean temperature are presented. The evaporation of the pure species droplet obeys to the D^2-law, while the mean temperature of the pure species droplet is continuously increasing. When the heat flux from the surrounding gas due to convection, becomes equal to the heat flux due to evaporation, the temperature of the droplet reaches the wet bulb temperature. The size reduction of the pure decane slightly deviates from the D^2-law at the initial stages of the evaporation process, due to initial droplet heat-up. For low evaporation rate conditions, the evaporation of the mixtures exhibits a distillation-type behaviour as also remarked by [37].

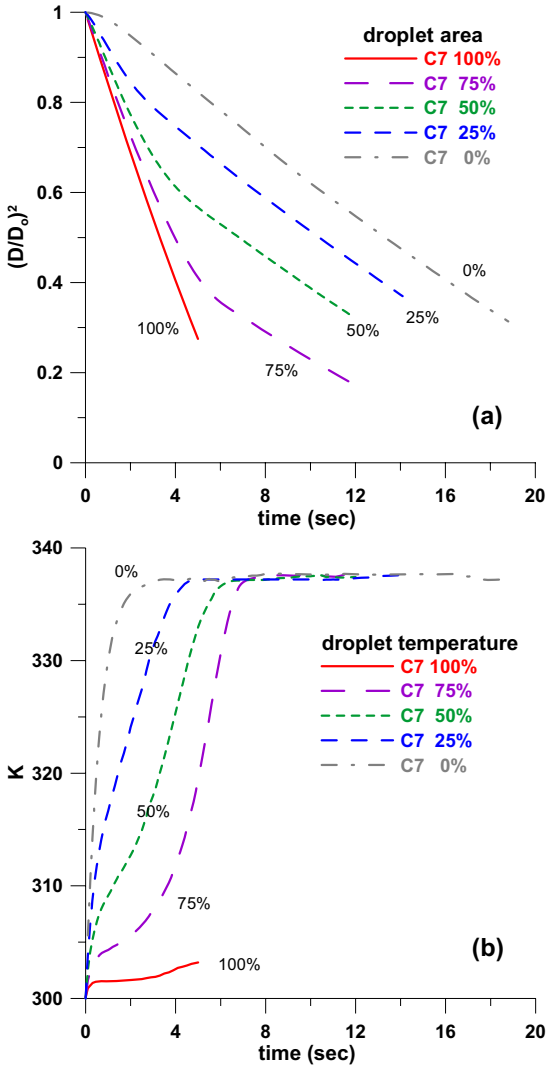

Figure 2: Predicted temporal evolution of (a) droplet's size and (b) droplet's mean temperature, showing the influence of the initial concentration in n-heptane.

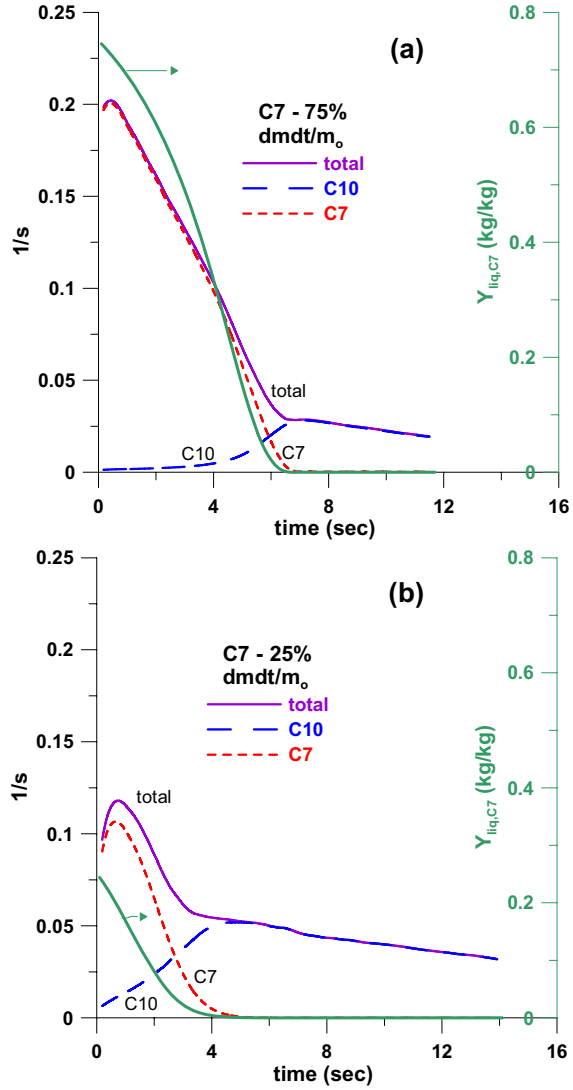

Figure 3: Temporal evolution of the evaporation rate (left axis) and mean liquid concentration (right axis) for the (a) 75% n-heptane mixture and (b) 25% n-heptane mixture.

Focusing on the 75% mixture (reference case), the droplet surface area reduction can be divided in two stages, which both obey the D^2-law. The evaporation of the volatile heptane, dominates the process at the first stages. During that period, a linear reduction of the surface area of the droplet with time is observed and the droplet's temperature initially increases with time with a decreasing rate, tending to reach a wet bulb temperature. Simultaneously, the concentration of the more volatile component decreases and after a short period of time, the less volatile decane starts to evaporate and the droplet is further heated. The slope of the droplet surface area versus time changes and it becomes constant after a transitional period. When the volatile component has been completely vaporized, the droplet reaches the wet bulb temperature which is that of pure decane at the given conditions.

This transitional behaviour is enhanced with increasing initial concentration in volatile n-heptane. The mixture of 75% n-heptane exhibits an intense transitional behaviour, while the 25% n-heptane mixture exhibits a weak transitional behaviour. These remarks and also be justified examining the temporal evolution of the evaporation of these two mixtures, shown in Figure 3.

Another interesting point that deserves to be addressed is related to the influence of the species diffusion term for multi-component mixtures of the energy equation (2):

$$\nabla \cdot \left(\sum_k \rho c_{P,k} T D_{k,m} \nabla Y_k \right) \qquad (3)$$

This term, must be included in the energy equation even though a single component droplet is simulated, since the surrounding gas is a mixture of air and vapour. The influence of ignoring this term in single component droplets is shown in Figure 4. As seen in comparison with Figure 2b, when ignoring this term, the wet bulb temperature of pure decane is different from the wet bulb temperature of mixture droplets consisting of heptane and decane independently of the initial concentration in heptane. This behaviour should not appear since the heptane is preferentially evaporated and at the later stages of droplet evaporation, the droplet is consisting of pure decane (Figure 3). When only the less volatile decane has left, droplet's temperature should reach pure decane's wet bulb temperature, as expected (Figure 2b).

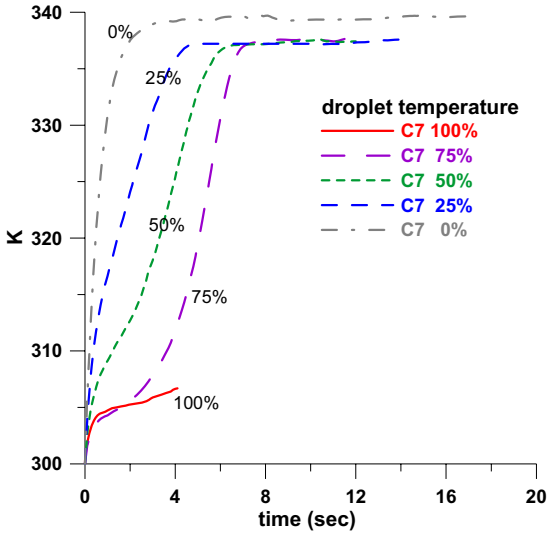

Figure 4: Influence of ignoring the species diffusion term in energy equation for single component droplets.

Flow field regimes

In this section the flow field distribution and the underlying transport processes are discussed in more detail. The following figures refer to the reference case of 75% initial mass concentration of n-heptane inside the droplet. In the upper part of Figure 5 the spatial distribution of the velocity magnitude non-dimensionalised with the free stream velocity can be seen, while in the lower part the streamlines in the liquid and gaseous phases are shown. Over the droplet, the flow is accelerated approximately 10% relative to the inlet velocity, while in the recirculation zone downstream of the droplet, velocities lower than 15% are found; the recirculation zone extends to a region of approximately one droplet diameter. Another recirculation with the same direction of rotation is formed inside the liquid phase and the velocities found inside the liquid mass are less than 10% of the free stream velocity, which is in accordance with the remarks of [2]. The physical processes which are taking place in the two phases, are effected by these two recirculation zones and they will be further discussed.

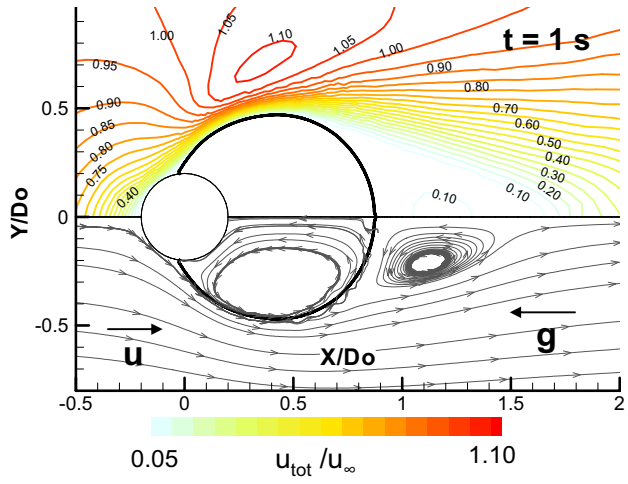

Figure 5: Total velocity magnitude (upper part) and streamlines (lower part) for the reference case

In Figure 6 the predicted gas phase isotherms are shown at various time instants for the reference case. Due to the convective character of the flow, isotherms at the front of the droplet are close to each other and a thermal boundary layer develops without any appreciable changes in its thickness with time. Downstream the droplet, a spatial distribution of the isotherms is formed due to the recirculation in the gaseous phase and the temperature wake becomes shorter in time.

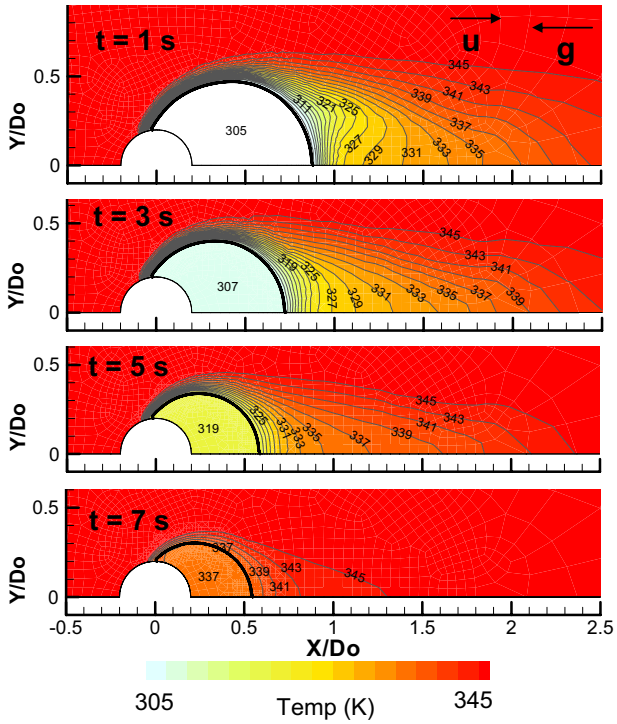

Figure 6: Temperature field (reference case)

Continuing the gas phase analysis, results for the vapour concentration field for the reference case are reported in Figure 7. The vapour pressure divided by the saturation vapour pressure of each component at the same cell temperature is plotted, which is more convenient instead of plotting the mass fraction of each component in the gaseous phase, which exhibit very different values due to pure species volatility difference. The upper part corresponds to n-decane vapour pressure non-dimensionalised with its saturation pressure in each computational cell; the lower part presents the same magnitude for n-heptane. Values of this relative saturation ratio can not exceed the corresponding values of liquid molecular fraction of each component. At the initial stage, the more volatile n-heptane dominates the evaporation process and exhibits large values at the gas-liquid interface region which progressively decrease; the opposite behaviour is observed for the less volatile n-decane component. In the interface region, strong concentration gradients are found and the spatial distribution of the relative saturation ratio for the two components, follow the same topology.

In Figure 8 the temperature field (upper part) and the n-heptane concentration field (lower part) inside the liquid droplet are presented for the reference case at various time instants. In this figure, the difference of each magnitude from the corresponding mean value of each magnitude at the same time is plotted, together with the corresponding mean mass averaged value for temperature and heptane concentration.

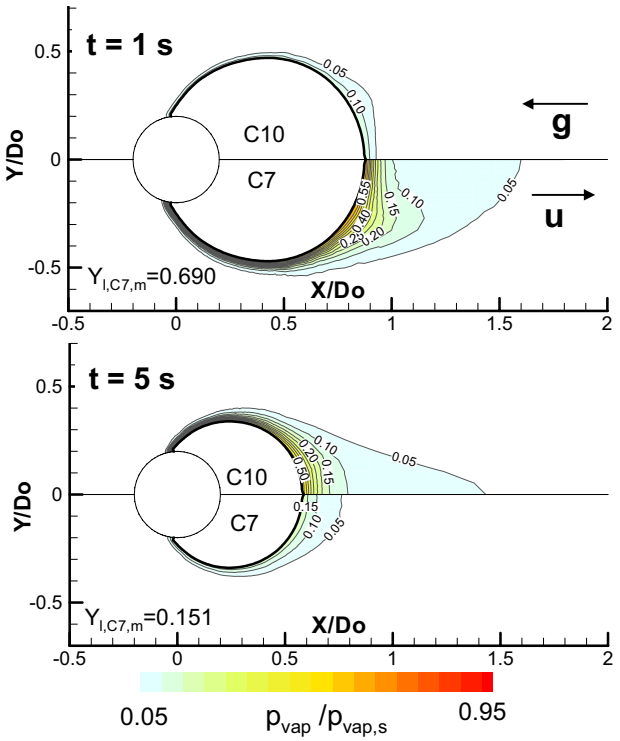

Figure 7: Vapour pressure field non-dimensionalised with saturation pressure for each species for n-decane (upper part) and n-heptane (lower part) for the reference case.

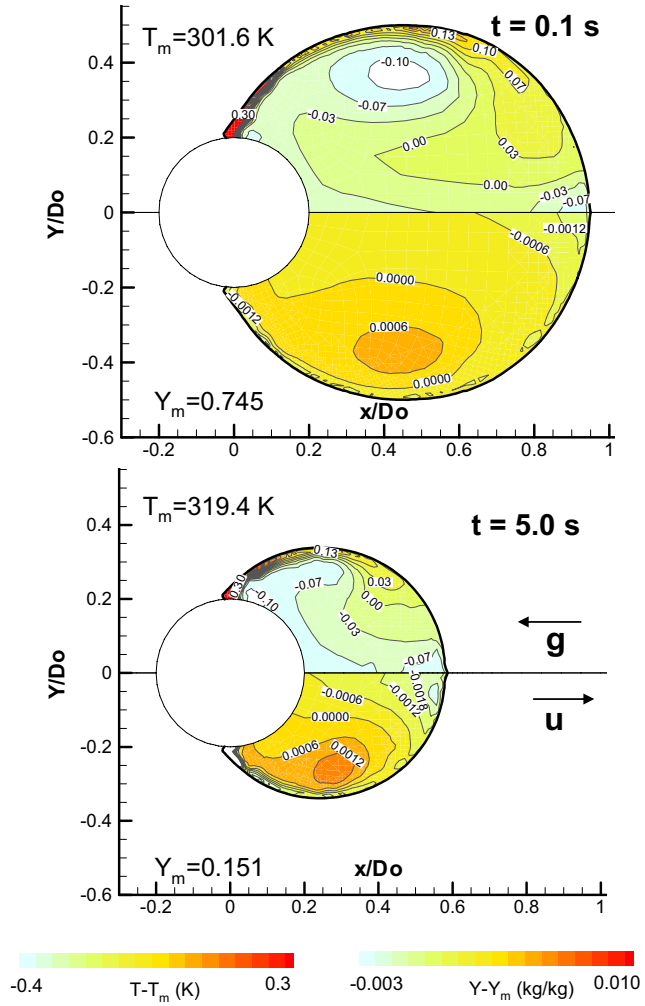

Figure 8: Temperature field (upper part) and concentration field (lower part) inside the liquid phase (reference case).

As seen, the relatively low evaporation rate in combination with the internal liquid circulation (Figure 5) which stirs the liquid phase and tends to homogenize the flow variables, results in small differences from the mean values for the temperature and the n-heptane concentration inside the liquid. On the other hand, small temperature and concentration differences imply that neglecting the Marangoni effect on surface tension is a reasonable hypothesis, while infinite conductivity and infinite diffusivity models could be used for fast predictions. In accordance with the numerical study of [18], inside the liquid core, a portion of the volatile n-heptane is entrapped throughout the evaporation process until it is fully evaporated, which is a result of the combination of the internal liquid circulation with the diffusion of heptane in the liquid mass.

CONCLUSIONS

The VOF methodology coupled with an evaporation model has been used to predict the evaporation process of a droplet consisting of one or two components at various concentrations and using an unstructured computational grid. The droplet was suspended in the spherical extremity of a capillary tube under convective flow conditions. The model used, has been first validated against experimental data, both for a single and a binary droplet, showing good agreement. The components of the binary droplet exhibit preferential evaporation and the surface reduction of the multi-component droplet is characterized by two stages which both follow the D^2-law. The temperature of a mixture droplet exhibits a transient behaviour; initially the droplet tends to reach a wet bulb temperature, followed by a heat-up and when the volatile n-heptane has been fully vaporised, droplet's temperature reaches the wet bulb temperature of pure n-decane. The more volatile species is entrapped in the interior of the liquid mass due to internal liquid circulation and species diffusion. A detailed description of the flow variables both in the gaseous and the liquid phases has been presented. Small temperature and concentration differences are found inside the liquid phase due to internal circulation, which justify the use of infinite conductivity and infinite diffusivity models for fast predictions.

ACKNOWLEDGMENT

This work has been partially supported by the Greek State Scholarships Foundation.

NOMENCLATURE

Symbol	Quantity	SI Unit
c_p	heat capacity	J/kg K
D	diameter	m
Dg	diffusion coefficient in gas	m^2/s
D_l	diffusion coefficient in liquid	m^2/s
g	gravity acceleration	m/s^2
k	thermal conductivity coefficient	W/mK
L	latent heat of vaporization	J/kg
m	mass	kg
T	temperature	K
t	time	s
u	velocity	m/s

Y	mass concentration	kg/kg

Greek Symbols

Symbol	Quantity	SI Unit
α	liquid volume fraction in cell	-
ρ	density	kg/m^3

subscripts

Symbol	Quantity
Q_{evap}	Q of evaporation
Q_g	Q in gas phase
Q_k	Q of k-species (mixture)
Q_l	Q in liquid phase
Q_m	Q in mixture or Q mean
Q_0	Q initial
Q_s	Q saturated
Q_{vap}	Q vapour

overscripts

Symbol	Quantity
$\dot{Q}$	rate of Q in time
Q^*	Q volumetric

abbreviations

C10	n-decane
C7	n-heptane
ECM	Effective Conductivity Model
FCM	Finite Conductivity Model
FDM	Finite Diffusivity Model
ICM	Infinite Conductivity Model
IDM	Infinite Diffusivity Model
VOF	Volume Of Fluid

REFERENCES

[1] R. Clift, J.R. Grace, M.E. Weber, *Bubbles, drops and particles*. 1978, New York: Academic Press.

[2] W.A. Sirignano, *Fluid Dynamics and Transport of Droplets and Sprays*. 1999: Cambridge University Press.

[3] R.B. Bird, W.E. Stewart, E.N. Lightfoot, *Transport Phenomena*. 2nd ed. 2002, New York: Wiley.

[4] S.D. Givler, J. Abraham, *Supercritical droplet vaporization and combustion studies.* Progress in Energy and Combustion Science, 1996. **22**(1): p. 1-28.

[5] R.S. Miller, K. Harstad, J. Bellan, *Evaluation of equilibrium and non-equilibrium evaporation models for many-droplet gas-liquid flow simulations.* International Journal of Multiphase Flow, 1998. **24**(6): p. 1025-1055.

[6] J. Bellan, *Supercritical (and subcritical) fluid behavior and modeling: drops, streams, shear and mixing layers, jets and sprays.* Progress in Energy and Combustion Science, 2000. **26**(4): p. 329-366.

[7] S.S. Sazhin, *Advanced models of fuel droplet heating and evaporation.* Progress in Energy and Combustion Science, 2006. **32**(2): p. 162-214.

[8] G.A.E. Godsave. *Burning of Fuel Droplets* in *4th International Symposium on combustion, The Combustion Institute*. 1953. Baltimore.

[9] D.B. Spalding. *The combustion of liquid fuels*. in *4th International Symposium on combustion, The Combustion Institute*. 1953. Baltimore.

[10] C.K. Law, *Unsteady droplet combustion with droplet heating.* Combustion and Flame, 1976. **26**: p. 17-22.

[11] C.K. Law, W.A. Sirignano, *Unsteady droplet combustion with droplet heating--II: Conduction limit.* Combustion and Flame, 1977. **28**: p. 175-186.

[12] B. Abramzon, W.A. Sirignano, *Droplet vaporization model for spray combustion calculations.* International Journal of Heat and Mass Transfer, 1989. **32**(9): p. 1605-1618.

[13] R.J. Haywood, R. Nafziger, M. Renksizbulut, *Detailed examination of gas and liquid phase transient processes in convective droplet evaporation.* Journal of Heat Transfer, 1989. **111**(2): p. 495-502.

[14] C.H. Chiang, M.S. Raju, W.A. Sirignano, *Numerical analysis of convecting, vaporizing fuel droplet with variable properties.* International Journal of Heat and Mass Transfer, 1992. **35**(5): p. 1307-1324.

[15] J.C. Lasheras, A.C. Fernandez-Pello, F.L. Dryer, *Experimental observations on the disruptive combustion of free droplets of multicomponent fuels.* Combustion science and technology, 1980. **22**(5-6): p. 195-209.

[16] C.K. Law, *Multicomponent droplet combustion with rapid internal mixing.* Combustion and Flame, 1976. **26**: p. 219-233.

[17] C.K. Law, *Internal boiling and superheating in vaporizing multicomponent droplets.* AIChE Journal, 1978. **24**(4): p. 626-632.

[18] C.M. Megaridis, W.A. Sirignano, *Numerical modeling of a vaporizing multicomponent droplet.* Symposium (International) on Combustion, 1990. **23**(1): p. 1413-1421.

[19] C.M. Megaridis, W.A. Sirignano, *Multicomponent droplet vaporization in a laminar convective environment.* Combustion Science and Technology, 1993. **87**(1-6): p. 27-44.

[20] H. Liu, E.J. Lavernia, R.H. Rangel, *Numerical simulation of substrate impact and freezing of droplets in plasma spray processes.* Journal of Physics D: Applied Physics, 1993. **26**(11): p. 1900-1908.

[21] M. Pasandideh-Fard, R. Bhola, S. Chandra, J. Mostaghimi, *Deposition of tin droplets on a steel plate: simulations and experiments.* International Journal of Heat and Mass Transfer, 1998. **41**(19): p. 2929-2945.

[22] L.L. Zheng, H. Zhang, *An adaptive level set method for moving-boundary problems: Application to droplet spreading and solidification.* Numerical Heat Transfer Part B-Fundamentals, 2000. **37**(4): p. 437-454.

[23] M. Pasandideh-Fard, S. Chandra, J. Mostaghimi, *A three-dimensional model of droplet impact and solidification.* International Journal of Heat and Mass Transfer, 2002. **45**(11): p. 2229-2242.

[24] R. Ghafouri-Azar, S. Shakeri, S. Chandra, J. Mostaghimi, *Interactions between molten metal droplets impinging on a solid surface.* International Journal of Heat and Mass Transfer, 2003. **46**(8): p. 1395-1407.

[25] D.J.E. Harvie, D.F. Fletcher, *A hydrodynamic and thermodynamic simulation of droplet impacts on hot surfaces, Part II: validation and applications.* International Journal of Heat and Mass Transfer, 2001. **44**(14): p. 2643-2659.

[26] D.J.E. Harvie, D.F. Fletcher, *A hydrodynamic and thermodynamic simulation of droplet impacts on hot surfaces, Part I: theoretical model.* International Journal of Heat and Mass Transfer, 2001. **44**(14): p. 2633-2642.

[27] N. Nikolopoulos, A. Theodorakakos, G. Bergeles, *A numerical investigation of the evaporation process of a liquid droplet impinging onto a hot substrate.* International Journal of Heat and Mass Transfer, 2007. **50**(1-2): p. 303-319.

[28] G. Strotos, M. Gavaises, A. Theodorakakos, G. Bergeles, *Numerical investigation on the evaporation of droplets depositing on heated surfaces at low Weber numbers.* International Journal of Heat and Mass Transfer, 2008. **51**(7-8): p. 1516-1529.

[29] G. Strotos, M. Gavaises, A. Theodorakakos, G. Bergeles. *Evaporation of a suspended multicomponent droplet under convective conditions*. in *ICHMT*. 2008. Marrakech, Morocco.

[30] A. Daïf, M. Bouaziz, X. Chesneau, A. Ali Cherif, *Comparison of multicomponent fuel droplet vaporization experiments in forced convection with the Sirignano model.* Experimental Thermal and Fluid Science, 1999. **18**(4): p. 282-290.

[31] C.W. Hirt, B.D. Nichols, *Volume of Fluid (Vof) Method for the Dynamics of Free Boundaries.* Journal of Computational Physics, 1981. **39**(1): p. 201-225.

[32] O. Ubbink, *Numerical prediction of two fluid systems with sharp interfaces*. 1997, PhD Thesis, Department of Mechanical Engineering, Imperial College of Science, Technology & Medicine,University of London.

[33] J.U. Brackbill, D.B. Kothe, C. Zemach, *A continuum method for modeling surface tension.* Journal of Computational Physics, 1992. **100**(2): p. 335-354.

[34] A. Theodorakakos, G. Bergeles, *Simulation of sharp gas-liquid interface using VOF method and adaptive grid local refinement around the interface.* International Journal for Numerical Methods in Fluids, 2004. **45**(4): p. 421-439.

[35] N. Nikolopoulos, A. Theodorakakos, G. Bergeles, *Normal impingement of a droplet onto a wall film: a numerical investigation.* International Journal of Heat and Fluid Flow, 2005. **26**(1): p. 119-132.

[36] G. Strotos, M. Gavaises, A. Theodorakakos, G. Bergeles, *Numerical investigation of the cooling effectiveness of a droplet impinging on a heated surface.* International Journal of Heat and Mass Transfer, 2008. **In Press**.

[37] I. Gökalp, C. Chauveau, H. Berrekam, N.A. Ramos-Arroyo, *Vaporization of miscible binary fuel droplets under laminar and turbulent convective conditions.* Atomization and Sprays, 1994. **4**: p. 661-676.